

1 **Title**

2 Human infant EEG recordings for 200 object images presented in rapid visual streams.

3 **Authors**

4 Tijl Grootswagers^{1,3}, Genevieve L Quek¹, Zhen Zeng^{1,2}, Manuel Varlet^{1,4}

5

6 **Affiliations**

7 1. The MARCS Institute for Brain, Behaviour and Development, Western Sydney University, Sydney,
8 Australia

9 2. Department of Linguistics and Modern Languages, The Chinese University of Hong Kong, Sha Tin,
10 Hong Kong SAR, China

11 3. School of Computer, Data, and Mathematical Sciences, Western Sydney University, Sydney, Australia

12 4. School of Psychology, Western Sydney University, Sydney, Australia

13

14 Corresponding author: Tijl Grootswagers (t.grootswagers@westernsydney.edu.au)

15 **Abstract**

16 Understanding the neural basis of human object recognition and semantic knowledge has
17 been a significant area of exploration, with recent focus aiming to reveal the developmental
18 trajectory of this core brain function. At present, however, there is limited access to high-
19 quality neuroimaging data obtained from human infants. Addressing this gap, we present a
20 dataset comprising electroencephalography responses from 42 human infants obtained in
21 response to visual presentations of various objects. Leveraging a rapid serial visual
22 presentation paradigm, 42 infants between 2 and 12 months of age viewed 200 images
23 spanning 50 distinct objects, with as many repetitions as possible tailored to individual infants'
24 comfort. Our technical validation demonstrates discernible neural responses to both
25 individual objects and categorical distinctions, affirming the dataset's robustness and utility
26 for exploring the neural underpinnings of visual object recognition in infancy. Building upon
27 insights gained from adult studies, our findings suggest that fast presentation paradigms hold
28 promise for efficiently capturing electrophysiological responses to a large array of visual
29 stimuli in human infants. This dataset represents a valuable resource for advancing our
30 understanding of the developmental trajectory of object recognition and semantic knowledge
31 in the early stages of human life.

32 **Background & Summary**

33 Our daily lives involve rapid and accurate visual recognition of a vast array of different objects,
34 such as faces, cars, trees, structures, animals, and many more. We are adept at recognising
35 individual objects even in cluttered visual environments (e.g., a messy kitchen), and in the face
36 of dramatic differences in an object's retinal projection caused by lighting conditions or
37 viewing angle. Understanding the neural basis of this impressive capacity has been a core
38 theme in cognitive neuroscience research^{1–4}, with an increasing number of papers aimed at
39 understanding how these capabilities develop during the earliest stages of life – human
40 infancy^{5–9}. While early findings in these neuroimaging infant studies have been promising,
41 stimulus set sizes and sample sizes have been relatively modest, and infant neural data is often
42 not publicly available. This is a barrier to progress in the field, particularly since the often noisy
43 quality of infant neuroimaging data necessitates a higher degree of preprocessing than
44 corresponding adult data would^{5,10,11}, and developing optimised preprocessing pipelines relies
45 on open data availability. Therefore, there is a pressing need for high-quality open-access
46 neuroimaging data associated with infant object recognition.

47

48 Collecting neurophysiological datasets on infants presents several challenges: Typically, classic
49 object vision experiments present around one image per second^{12–14}. Thus, obtaining multiple
50 trials for many images can thus take many hours, which is infeasible to achieve with infants
51 who cannot tolerate long experiments. However, we have recently shown in adult participants
52 that it is possible to uncover overlapping information about visual stimuli presented in rapid
53 serial visual presentation (RSVP) streams using electroencephalography (EEG)^{15–18}. In these
54 studies, 5 minutes of EEG recording can comprise more than 1000 visual object presentations
55 appearing at a rate of 5 images per second. Multivariate pattern classification analysis of this
56 data revealed detailed temporal dynamics of object processing that are similar to those
57 documented by studies using slower presentation speeds. Therefore, fast presentation
58 paradigms may be highly suitable for collecting neural responses to large numbers of visual
59 object stimuli in infant populations.

60
61 Here, we present a dataset of human infant (n=45) EEG responses to 200 object images
62 spanning 50 individual categories (e.g., dog, hammer, chair etc.). Each image was repeated at
63 least 3 times for each participant, with the experiment lasting as long as the infant participant
64 could comfortably comply. We used the same rapid serial visual presentation paradigm as a
65 previous adult study¹⁵. Participants' age range covered the major developmental changes in
66 the visual system in the first year of life^{8,19–22}, providing an unprecedented opportunity to
67 investigate the development of vision in humans. Technical validation was carried out to probe
68 general age-related effects and infant-adult comparison in object recognition in infancy.
69 Results indicate distinguishable neural responses to object categories in infants over 6 months
70 old and less matured responses in infants up to 6 months old, demonstrating that the dataset
71 can serve as a high-quality resource for future investigations into the neural development of
72 visual object recognition.

73 **Methods**

74 A total of 42 infants took part in the experiment, recruited via the MARCS Institute BabyLab
75 database at Western Sydney University. Each caregiver was briefed on experimental
76 procedures and provided their informed consent prior to the start of the experiment, including
77 written consent for publishing the anonymised data. Participants were 16 female and 26 male
78 human infants, mean age 6.57 months (sd 3.02 months), age range 1.8 – 11.5 months (Figure
79 1). We recorded demographic information about each participant's language and education
80 background. All participants had been screened for normal hearing and vision and had no
81 known medical issues. There are 8 participants marked for potential exclusion due to notably
82 poor signal quality or equipment failure (marked in the *participants.tsv* file). These participants
83 are included in the release for completeness, and in the technical validation reported here. All
84 aspects of the study were approved by the Western Sydney University ethics committee
85 (H14498).

86

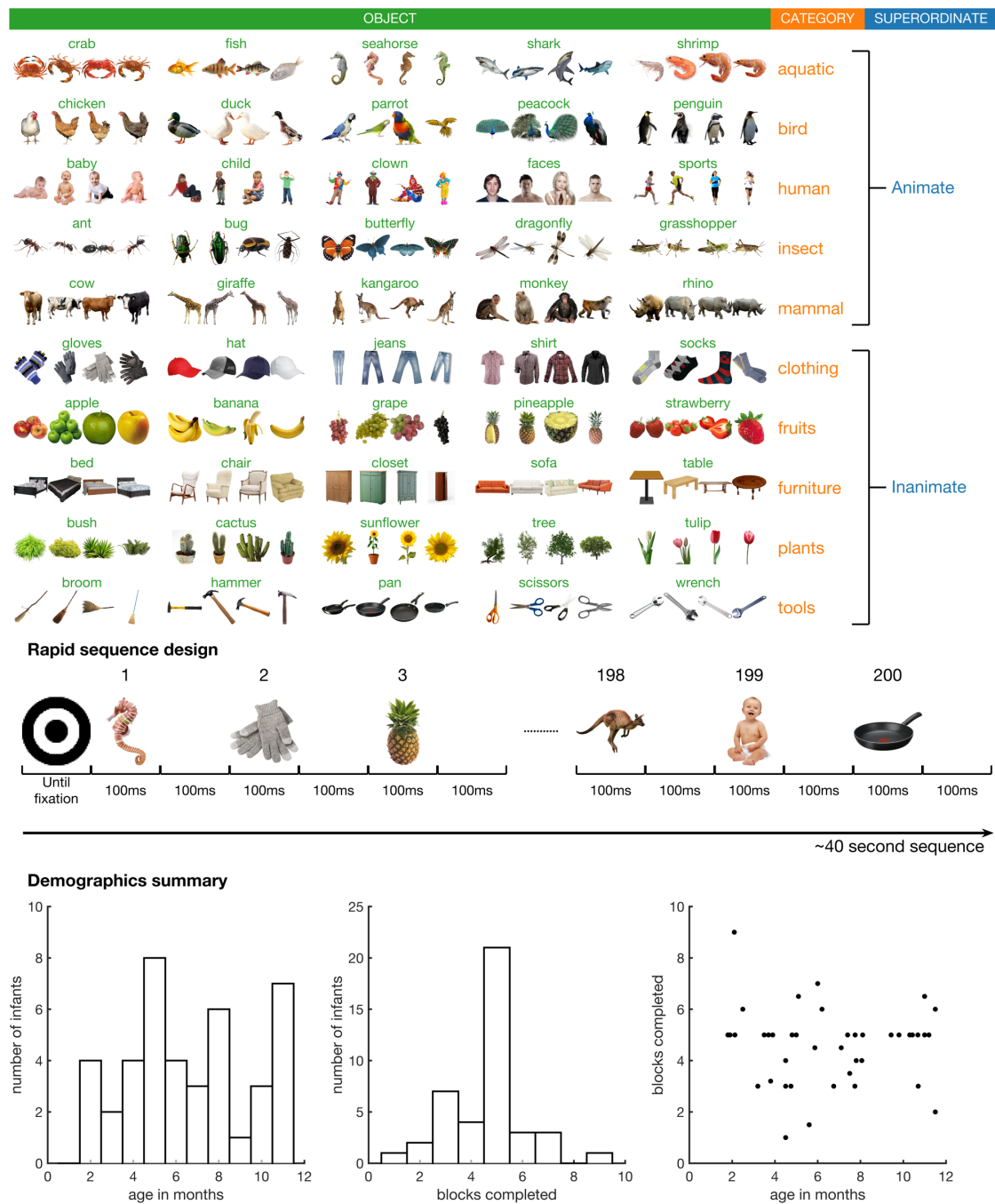


Figure 1: Stimuli, design, and demographics. Top: Stimulus set used in the experiment, adapted from¹⁵. Middle: Rapid serial visual presentation design, showing part of a rapid sequence of stimuli. Bottom: Key demographic information including age in months, number of blocks completed (200 image presentations in each block), and a scatter plot of age by blocks completed.

Stimuli were taken from a previous object recognition study¹⁵ (Figure 1), and consisted of 200 images spanning 50 object concepts. Each stimulus was associated with three levels of labels. The first level corresponded to the individual object (e.g., dog, apple, hammer, etc.), the second level corresponded to the category (e.g., mammal, fruit, tool, etc.) and the third level corresponded to the superordinate category (e.g., animate or inanimate). The experiment was programmed in Python (v3.7), using the Psychopy²³ library (version 3.0.5). Images appeared in randomised order in sequences at a rate of exactly 5Hz with a 50% duty cycle (Figure 1), that is, each image appeared for 100ms followed by a 100ms blank screen. Each 40 second sequence contained one presentation of each unique stimulus. Participants sat on their

103 caregiver's lap in a dimly lit experiment booth approximately 57cm from the screen, so that
 104 each stimulus subtended approximately 6 degrees visual angle. A fixation bullseye (0.5 degrees
 105 visual angle) was overlaid at the centre of each image. To promote the infant's attention and
 106 engagement to the screen, before each sequence, the bullseye alternately increased and
 107 decreased in size until the experimenter manually started the sequence after verifying that
 108 the infant was looking at the screen. The experiment was paused when the infant was looking
 109 away and resumed when the infant's attention was directed back to the screen. The
 110 experiment lasted between approximately 5 minutes to 20 minutes, depending on the infant's
 111 compliance. On average, infants completed 4.58 full sequences (sd 1.48).

112
 113 We used a BrainVision Liveamp EEG amplifier and Psychopy²³ stimulus presentation with
 114 Labstreaminglayer connector protocol²⁴ (<https://labstreaminglayer.org/>) for wireless EEG
 115 recording (Figure 1B). Specifically, a Brain Products Liveamp server software
 116 (<https://github.com/brain-products/LSL-LiveAmp>) was used on the EEG recording computer
 117 to wirelessly connect to the Liveamp amplifier. An event trigger coding for the stimulus
 118 number was sent for each image presentation using Psychopy on a stimulus presentation
 119 computer. On the EEG recording computer, a Labstreaminglayer recorder software
 120 (<https://github.com/labstreaminglayer/App-LabRecorder>) was used to wirelessly detect the
 121 signal streams from both the EEG amplifier and the stimulus presentation triggers, and
 122 visualise ongoing signals during EEG recording. We used BrainVision RNet caps with 32
 123 electrodes, arranged according to the international standard 10–10 system for electrode
 124 placement^{25,26}. The signal was digitised at a 500Hz sample rate.

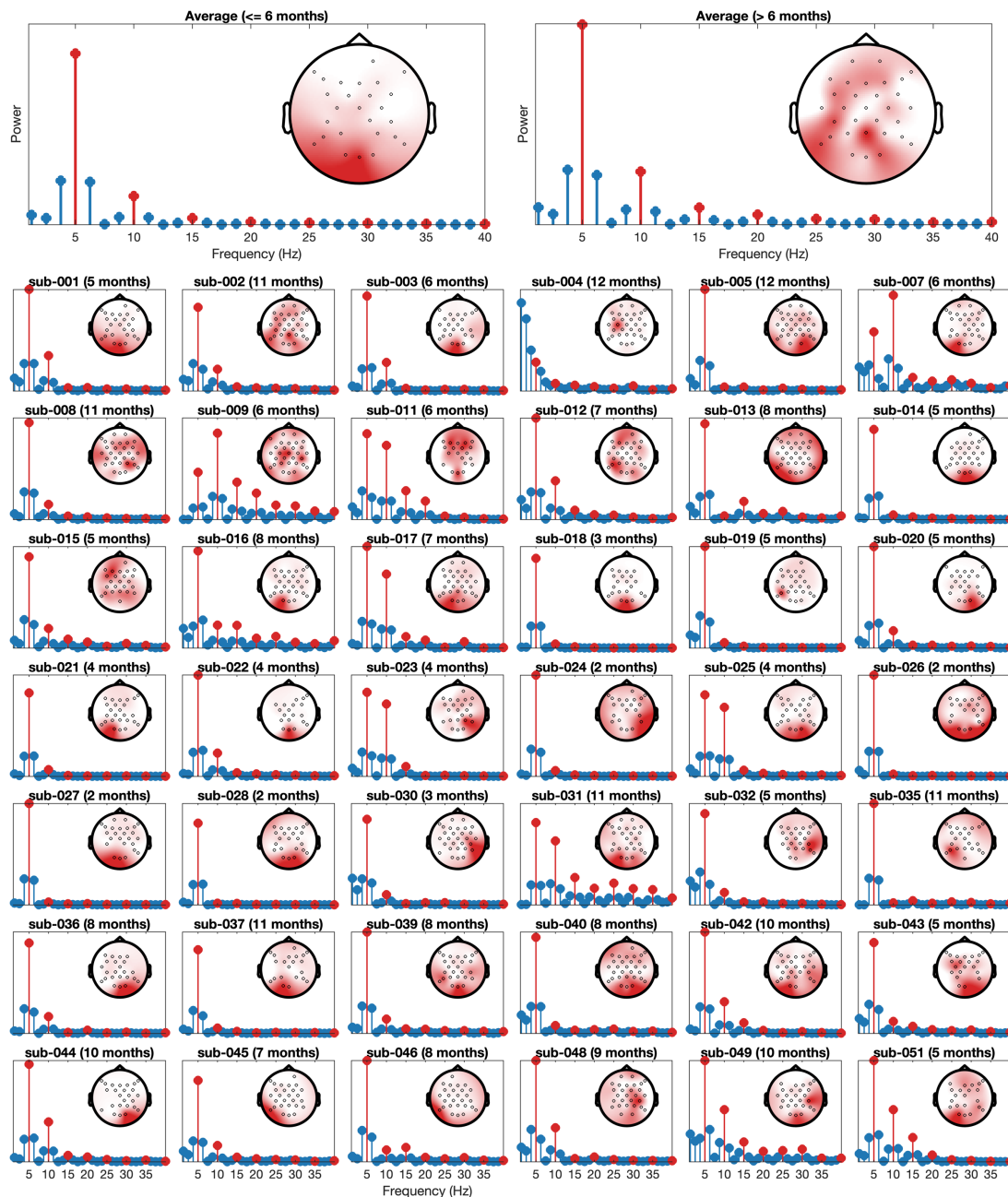
125 Data Records

126 All data and code reported here are publicly available²⁷. The raw infant EEG recordings are
 127 formatted according to the BIDS^{28,29} standard and hosted on OpenNeuro
 128 (<https://doi.org/10.18112/OPENNEURO.DS005106.v1.1.0>)²⁷. The preprocessed data,
 129 individual RDMs, and RSA results are included for convenience, as well as the custom Matlab
 130 code to generate the technical validation figures in this paper. The data repository contains
 131 instructions and example code on how to get started with analyses²⁷.

132 Technical Validation

133 We performed basic quality checks and technical validation for each subject individually by
 134 examining signal amplitude in the frequency domain, and by using a standard multivariate
 135 pattern analysis in the time-domain¹⁰. Note that this pipeline is not made to be an optimal
 136 analysis of the potential of the dataset, but its goal is to validate the presence of condition-
 137 specific information.

138
 139 We applied the clean_rawdata preprocessing pipeline (see provided analysis code) from the
 140 EEGLab (v2023.0) toolbox³⁰ in Matlab (R2023b). This automated pipeline includes a 0.5Hz
 141 highpass filter, bad segment deletion (which resulted in an average exclusion of 1.5% of
 142 epochs per infant), and bad channel deletion (average 6.5 channels per infant). In addition,
 143 data were filtered using a Hamming windowed FIR 40Hz lowpass filter and re-referenced to
 144 the average reference. Epochs were then created for each individual stimulus presentation
 145 ranging from [-100 to 800ms] relative to stimulus onset. No further preprocessing steps were
 146 applied for the analyses presented here.



148

149 **Figure 2:** Averaged (top left for the younger, and top right for the older group) and individual
 150 power spectrum. The 5Hz presentation frequency and harmonics (10Hz, 15Hz, 20Hz, etc)
 151 shown in red. Insets in each plot are the channel topographies of the 5Hz response.

152

153 We then used the fieldtrip³¹ toolbox (version 20230926) to compute the power spectrum
 154 between 0-40 Hz using a Fast Fourier Transform (FFT) with a fixed length Hanning window of
 155 0.8s yielding a frequency resolution of 1.25Hz. We averaged the frequency spectra across
 156 epochs for each infant, to examine their neural response at the 5Hz presentation rate and its
 157 corresponding harmonics. Figure 2 confirms that in most infants, a strong 5Hz signal
 158 originating from occipital electrodes can be observed.

159

160 To test for condition-related information in the EEG responses, we performed time-resolved
 161 representational similarity analyses^{10,32} in Matlab using the CoSMoMVPA toolbox³³. First, we
 162 created RDMs for each infant by baseline-correcting and PCA-transforming the data from
 163 posterior electrodes (C3, CP5, CP1, Pz, P3, P7, P9, O1, Oz, O2, P10, P8, P4, CP2, CP6, C4, Cz),
 164 averaging the PCA transformed responses to each of the 200 images, and computing the

165 dissimilarity (1-pearson correlation) between each pair of images, separately for each time
166 point in the epochs. This yielded a 200 by 200 representational dissimilarity matrix (RDM) for
167 each time point for each infant. To probe general developmental effects for the purpose of
168 the technical validation, instead of a more granular age analysis, we averaged the infant data
169 into two groups: up to 6 months, and over 6 months. To estimate categorical information in
170 the infant and adult RDMs, we created binary model RDMs at three levels (object, category,
171 and animacy) that represented same (0) or different (1) content, and computed the Spearman
172 correlation between the lower triangles (excluding the diagonal) of the model and the neural
173 RDMs at each time point^{10,15,32}. Associated p-values were corrected for multiple comparisons
174 across time points using the False Discovery Rate (FDR)³⁴ with a q-value at 0.05. Results
175 indicated decodable information about the categorical levels in infants over 6 months but non-
176 significant decoding in infants up to 6 months (Figure 3). Decoding results from the older group
177 but not the younger group showed a comparable temporal dynamics to adult EEG
178 representations obtained previously with the same 200 object stimuli and 5Hz rapid stimulus
179 presentation¹⁵ (see original publication for further details).

180
181 Finally, we evaluated how well our infant RDMs overlapped with those from this existing
182 openly available adult EEG dataset¹⁵. For analysing the structural overlap between infant and
183 adult data, we performed a time-time Spearman correlation between the two averaged infant
184 RDMs (up to 6 months, and over 6 months) and the mean adult RDMs at each pair of time
185 points, resulting in a time-time correlation matrix. We then calculated cluster-based p-values
186 by shuffling the RDMs 1000 times and re-computing the time-time correlations, applied a
187 cluster-forming threshold of $p < 0.05$ and calculated the maximum cluster sum statistic for each
188 permutation. We then reported the clusters in the original correlation result that exceeded
189 95% of the max-statistic permutation distribution. Figure 3 shows that for the up to 6 month
190 olds, no adult-infant-correlations survived multiple comparison correction. However, the over
191 6 months olds showed a cluster of shared variance in the representational structures of the
192 two groups spanning approximately 400-500ms in the infant data to 150-250ms in the adult
193 data (Figure 3).

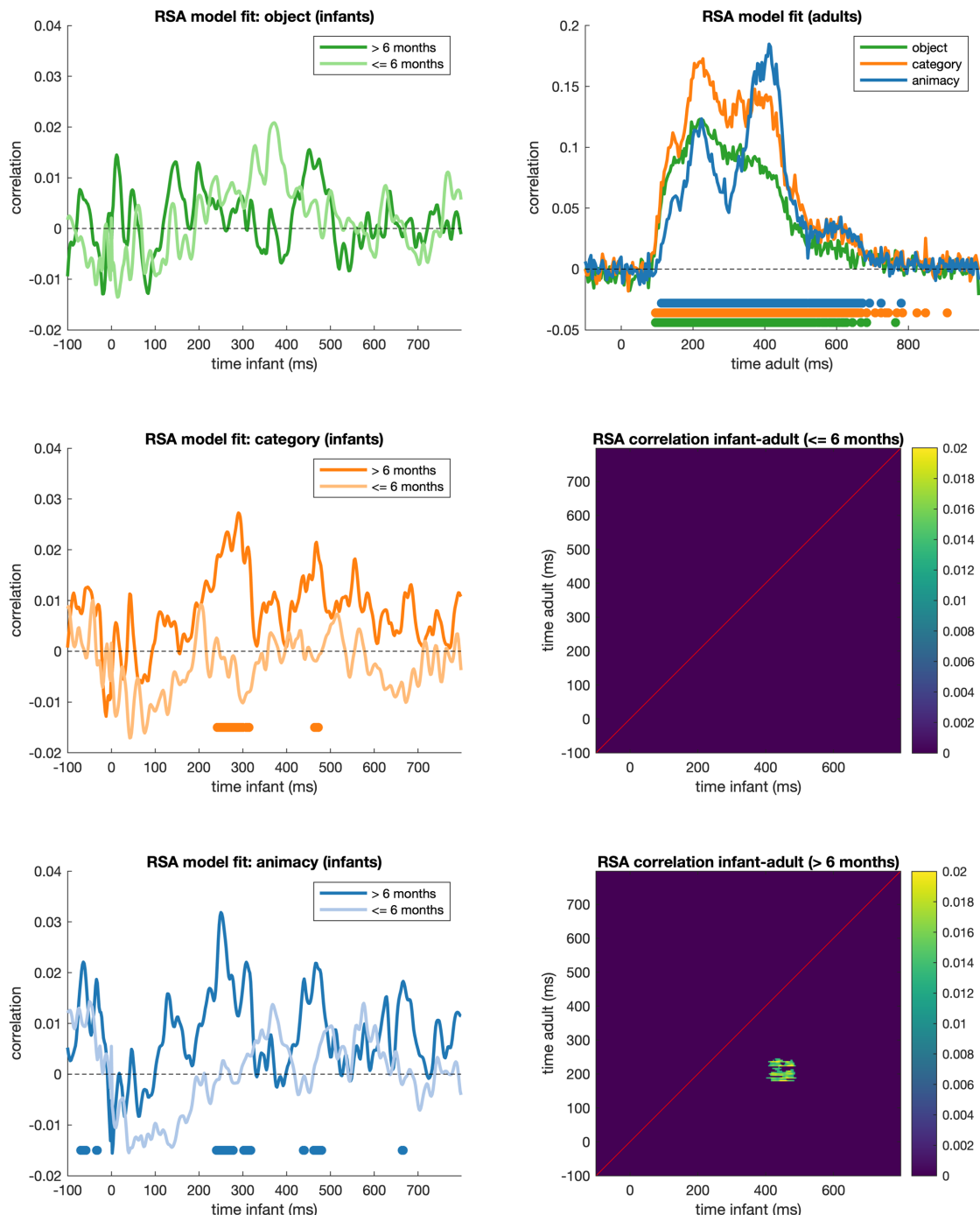


Figure 3: Time-varying Representational Similarity Analysis (RSA) results. Left: RSA model fits for the infant RDM for 3 categorical levels, split by age group. Marks above the x-axis indicate $p < 0.05$ (FDR corrected). Top-right: RSA model fits for the adult RDMs for comparison, with marks above the x-axis indicating $p < 0.05$ (FDR corrected). Bottom-right: Time-time correlation matrices between the two infant groups and adult RDMs, thresholded at $p < 0.05$ (cluster-corrected). The significant cluster below the diagonal suggest that object representations arising during later stages of the older infant response (400–500ms) significantly correlated to an early stage of the adult neural response (150–250ms).

Code Availability

Code and detailed instructions to reproduce the technical validation analyses and figures presented in this manuscript are available in the “code” directory in the abovementioned OpenNeuro repository²⁷.

207 **Acknowledgements**

208 This research was supported by ARC DE230100380 (TG) and ARC DP220103047 (MV).

209 **Author contributions**

210 TG: Conceptualization, Methodology, Software, Investigation, Formal analysis, Visualization,
211 Data Curation, Writing – Original Draft, Writing – Review & Editing, Project administration,
212 Funding Acquisition.
213 GQ: Conceptualization, Methodology, Investigation, Formal analysis, Data Curation, Writing –
214 Original Draft, Writing – Review & Editing.
215 ZZ: Investigation, Software, Formal analysis, Data Curation, Writing – Review & Editing.
216 MV: Methodology, Writing – Review & Editing, Funding Acquisition.

217 **Competing interests**

218 The authors declare no competing interests.

219 **References**

- 220 1. Wardle, S. G. & Baker, C. Recent advances in understanding object recognition in the
221 human brain: deep neural networks, temporal dynamics, and context. *F1000Research* **9**,
222 590 (2020).
- 223 2. DiCarlo, J. J. & Cox, D. D. Untangling invariant object recognition. *Trends Cogn. Sci.* **11**,
224 333–341 (2007).
- 225 3. Gauthier, I. & Tarr, M. J. Visual Object Recognition: Do We (Finally) Know More Now Than
226 We Did? <http://dx.doi.org/10.1146/annurev-vision-111815-114621>
227 <http://www.annualreviews.org/doi/10.1146/annurev-vision-111815-114621> (2016).
- 228 4. Robinson, A. K., Quek, G. L. & Carlson, T. A. Visual Representations: Insights from Neural
229 Decoding. *Annu. Rev. Vis. Sci.* **9**, null (2023).
- 230 5. Ashton, K. *et al.* Time-resolved multivariate pattern analysis of infant EEG data: A practical
231 tutorial. *Dev. Cogn. Neurosci.* **54**, 101094 (2022).
- 232 6. Bayet, L. *et al.* Temporal dynamics of visual representations in the infant brain. *Dev. Cogn.
233 Neurosci.* **45**, 100860 (2020).
- 234 7. Xie, S. *et al.* Visual category representations in the infant brain. *Curr. Biol.* (2022)
235 doi:10.1016/j.cub.2022.11.016.
- 236 8. Ayzenberg, V. & Behrmann, M. Development of visual object recognition. *Nat. Rev.
237 Psychol.* **3**, 73–90 (2024).
- 238 9. Peykarjou, S., Hoehl, S. & Pauen, S. The development of visual categorization based on
239 high-level cues. *Child Dev.* **n/a**.
- 240 10. Grootswagers, T., Wardle, S. G. & Carlson, T. A. Decoding Dynamic Brain Patterns from
241 Evoked Responses: A Tutorial on Multivariate Pattern Analysis Applied to Time Series
242 Neuroimaging Data. *J. Cogn. Neurosci.* **29**, 677–697 (2017).
- 243 11. Delorme, A. EEG is better left alone. *Sci. Rep.* **13**, 2372 (2023).
- 244 12. Carlson, T. A., Tovar, D. A., Alink, A. & Kriegeskorte, N. Representational dynamics of
245 object vision: The first 1000 ms. *J. Vis.* **13**, 1 (2013).
- 246 13. Cichy, R. M., Pantazis, D. & Oliva, A. Resolving human object recognition in space and time.
247 *Nat. Neurosci.* **17**, 455–462 (2014).
- 248 14. Kaneshiro, B., Guimaraes, M. P., Kim, H.-S., Norcia, A. M. & Suppes, P. A Representational
249 Similarity Analysis of the Dynamics of Object Processing Using Single-Trial EEG
250 Classification. *PLOS ONE* **10**, e0135697 (2015).
- 251 15. Grootswagers, T., Robinson, A. K. & Carlson, T. A. The representational dynamics of visual
252 objects in rapid serial visual processing streams. *NeuroImage* **188**, 668–679 (2019).
- 253 16. Grootswagers, T., Robinson, A. K., Shatek, S. M. & Carlson, T. A. Untangling featural and
254 conceptual object representations. *NeuroImage* **202**, 116083 (2019).

- 255 17. Grootswagers, T., Zhou, I., Robinson, A. K., Hebart, M. N. & Carlson, T. A. Human EEG
 256 recordings for 1,854 concepts presented in rapid serial visual presentation streams. *Sci.
 257 Data* **9**, 3 (2022).
- 258 18. Robinson, A. K., Grootswagers, T. & Carlson, T. A. The influence of image masking on object
 259 representations during rapid serial visual presentation. *NeuroImage* **197**, 224–231 (2019).
- 260 19. Ellis, C. T. *et al.* Retinotopic organization of visual cortex in human infants. *Neuron* **109**,
 261 2616–2626 (2021).
- 262 20. Siu, C. & Murphy, K. The development of human visual cortex and clinical implications. *Eye
 263 Brain Volume* **10**, 25–36 (2018).
- 264 21. Kovács, I. Human development of perceptual organization. *Vision Res.* **40**, 1301–1310
 265 (2000).
- 266 22. Dobson, V. & Teller, D. Y. Visual acuity in human infants: a review and comparison of
 267 behavioral and electrophysiological studies. *Vision Res.* **18**, 1469–1483 (1978).
- 268 23. Peirce, J. *et al.* PsychoPy2: Experiments in behavior made easy. *Behav. Res. Methods* **51**,
 269 195–203 (2019).
- 270 24. Kothe, C. *et al.* The lab streaming layer for synchronized multimodal recording. *bioRxiv*
 271 2024–02 (2024).
- 272 25. Jasper, H. H. The ten-twenty electrode system of the International Federation.
Electroencephalogr Clin Neurophysiol **10**, 371–375 (1958).
- 273 26. Oostenveld, R. & Praamstra, P. The five percent electrode system for high-resolution EEG
 275 and ERP measurements. *Clin. Neurophysiol.* **112**, 713–719 (2001).
- 276 27. Grootswagers, T., Quek, G., Zeng, Z. & Varlet, M. 200 Objects Infants EEG. Openneuro
 277 <https://doi.org/10.18112/OPENNEURO.DS005106.v1.1.0> (2024).
- 278 28. Gorgolewski, K. J. *et al.* The brain imaging data structure, a format for organizing and
 279 describing outputs of neuroimaging experiments. *Sci. Data* **3**, 160044 (2016).
- 280 29. Pernet, C. R. *et al.* EEG-BIDS, an extension to the brain imaging data structure for
 281 electroencephalography. *Sci. Data* **6**, 103 (2019).
- 282 30. Delorme, A. & Makeig, S. EEGLAB: an open source toolbox for analysis of single-trial EEG
 283 dynamics including independent component analysis. *J. Neurosci. Methods* **134**, 9–21
 284 (2004).
- 285 31. Oostenveld, R., Fries, P., Maris, E. & Schoffelen, J.-M. FieldTrip: Open Source Software for
 286 Advanced Analysis of MEG, EEG, and Invasive Electrophysiological Data. *Comput. Intell.
 287 Neurosci.* **2011**, 156869 (2010).
- 288 32. Kriegeskorte, N. & Kievit, R. A. Representational geometry: integrating cognition,
 289 computation, and the brain. *Trends Cogn. Sci.* **17**, 401–412 (2013).
- 290 33. Oosterhof, N. N., Connolly, A. C. & Haxby, J. V. CoSMoMVPA: Multi-Modal Multivariate
 291 Pattern Analysis of Neuroimaging Data in Matlab/GNU Octave. *Front. Neuroinformatics*
 292 **10**, (2016).
- 293 34. Benjamini, Y. & Hochberg, Y. Controlling the False Discovery Rate: A Practical and Powerful
 294 Approach to Multiple Testing. *J. R. Stat. Soc. Ser. B Methodol.* **57**, 289–300 (1995).
- 295